Cell Reports
Article

Single-Cell Profiling of Epigenetic Modifiers Identifies PRDM14 as an Inducer of Cell Fate in the Mammalian Embryo

Adam Burton,[1,6] Julius Muller,[2,6] Shengjiang Tu,[4] Pablo Padilla-Longoria,[3] Ernesto Guccione,[2,5,*] and Maria-Elena Torres-Padilla[1,*]

[1]Institut de Génétique et de Biologie Moléculaire et Cellulaire, CNRS/INSERM U964, Université de Strasbourg, F-67404 Illkirch, CU de Strasbourg, France

[2]Division of Cancer Genetics and Therapeutics, Laboratory of Chromatin, Epigenetics and Differentiation, Institute of Molecular and Cell Biology, Agency for Science, Technology and Research, Singapore 138673, Singapore

[3]Instituto de Investigaciones en Matemáticas Aplicadas y en Sistemas, Universidad Nacional Autónoma de México, C.U., Distrito Federal 04510, México

[4]Howard Hughes Medical Institute, Department of Biochemistry, New York University School of Medicine, 522 First Avenue, New York, NY 10016, USA

[5]Department of Biochemistry, Yong Loo Lin School of Medicine, National University of Singapore, Singapore 119228, Singapore

[6]These authors contributed equally to this work

*Correspondence: eguccione@imcb.a-star.edu.sg (E.G.), metp@igbmc.fr (M.-E.T.-P.)

http://dx.doi.org/10.1016/j.celrep.2013.09.044

SUMMARY

Cell plasticity or potency is necessary for the formation of multiple cell types. The mechanisms underlying this plasticity are largely unknown. Preimplantation mouse embryos undergo drastic changes in cellular potency, starting with the totipotent zygote through to the formation of the pluripotent inner cell mass (ICM) and differentiated trophectoderm in the blastocyst. Here, we set out to identify and functionally characterize chromatin modifiers that define the transitions of potency and cell fate in the mouse embryo. Using a quantitative microfluidics approach in single cells, we show that developmental transitions are marked by distinctive combinatorial profiles of epigenetic modifiers. Pluripotent cells of the ICM are distinct from their differentiated trophectoderm counterparts. We show that PRDM14 is heterogeneously expressed in 4-cell-stage embryos. Forced expression of PRDM14 at the 2-cell stage leads to increased H3R26me2 and can induce a pluripotent ICM fate. Our results shed light on the epigenetic networks that govern cellular potency and identity in vivo.

INTRODUCTION

Cell plasticity is essential for the formation of pluripotent cells and the development of multicellular organisms. However, the molecular mechanisms underlying cell plasticity are largely unknown.

The mammalian embryo undergoes major changes in cell plasticity before implantation, resulting in the generation of cells of different potencies. The tight regulation of such transitions in potency is essential to ensure the formation of the new organism. In mammals, development begins with the formation of the zygote following fusion of the gametes. Epigenetic reprogramming of the gametes after fertilization is necessary to restore full developmental plasticity in the newly formed embryo. The zygote is therefore a totipotent cell because it is able to produce all cell types in a new organism, including embryonic and extraembryonic tissues. Subsequent development is accompanied by a progressive narrowing of developmental potency and proceeds to the first lineage choice: the separation of the pluripotent inner cell mass (ICM) and the outer, more differentiated trophectoderm (TE) in the blastocyst. Thus, during the first 3 days of development, the mouse embryo comprises totipotent, pluripotent, and differentiated cells. The preimplantation mouse embryo provides a unique model for exploring the foundations of totipotency and differentiation in vivo.

Although lineage allocation between ICM and TE is only morphologically visible at the blastocyst stage, the first cell-differentiation event can be appreciated earlier, at the 8-cell stage, when individual blastomeres become polarized (Ziomek and Johnson, 1980). A number of subsequent asymmetric cell divisions from the 8- to 32-cell stage lead to the formation of distinct inner apolar and outer polar cells in the 16-cell morula and 32-cell-stage early blastocyst. The inside/outside position of the resulting cells correlates with subsequent lineage allocation to the ICM or TE, respectively, in the blastocyst (Johnson and McConnell, 2004). The TE is a functional epithelium that gives rise to extraembryonic tissues required for implantation, whereas the ICM cells retain their pluripotent character and subsequently form the primitive endoderm (PE) and the

epiblast (EPI), which gives rise to all cells of the developing embryo itself.

How the transitions in potency are regulated at the molecular level remains a crucial and poorly understood question in developmental and stem cell biology. A number of transcription factors (TFs) have been identified as critical for the maintenance of these lineages, including *Cdx2* for the TE, and *Nanog* and *Pou5f1*/*Oct4* for the ICM. However, *Nanog* and *Oct4* are not required for the initial lineage establishment to occur (Mitsui et al., 2003; Nichols et al., 1998). TE commitment occurs initially at the 32-cell stage, and concordantly *Cdx2* expression becomes restricted to outer cells at this point (Dietrich and Hiiragi, 2007; Strumpf et al., 2005). ICM commitment seems to occur later than TE commitment, during the 32- to 64-cell stages, although the core TFs associated with the identity of inner cells, *Nanog* and *Oct4*, undergo complete lineage restriction only one to two cell cycles later (Dietrich and Hiiragi, 2007; Guo et al., 2010). A recent study that analyzed the expression of TFs expressed at the single-cell level in early mouse embryos suggested that there is a gradient of expression among blastomeres of some TFs (e.g., *Sox2*) in the 16-cell morula stage (Guo et al., 2010).

The chromatin state of the TE and ICM lineages is expected to be crucial for their initial commitment and differentiation potential. Chromatin modifier complexes likely act to generate a chromatin environment that allows lineage-specific TFs to exercise their functions in cell-fate decisions. Furthermore, they also have the potential to transmit molecular changes across cell divisions. Notably, the epigenetic dynamics during mammalian preimplantation development are characterized by major changes in DNA methylation, histone modifications, and the incorporation of histone variants (Burton and Torres-Padilla, 2010; Hemberger et al., 2009). Other investigators (Parfitt and Zernicka-Goetz, 2010) and we (Torres-Padilla et al., 2007) have shown that the first differentiation events in the embryo can be orchestrated by histone modifications. In particular, we showed that methylation of arginine 26 in histone H3 (H3R26me2) by the protein arginine methyl transferase 4 (PRMT4/CARM1) can regulate cell fate. Collectively, these findings suggest that chromatin modifications and their modifiers play a crucial, but still poorly understood, role in the processes of reprogramming and differentiation during development.

Lineage-tracing approaches and micromanipulation of individual blastomeres have led to the general consensus that the fates of individual blastomeres are not fully determined until the blastocyst forms, implying that although two distinct lineages emerge at the 16-cell stage, embryonic cells retain plasticity and are not committed until the subsequent division occurs (Guo et al., 2010; Johnson, 2009). Therefore, single-cell gene-expression analysis of blastomeres during this transition can reveal previously unidentified patterns in the molecular composition of individual blastomeres, which may provide the foundations for cellular potency and lineage segregation.

In order to obtain insights into the epigenetic mechanisms behind cell potency and lineage segregation in the mouse embryo, we conducted simultaneous quantitative and combinatorial expression profiling of chromatin modifiers in single cells throughout preimplantation development using microfluidics technology. We show that developmental transitions are marked by distinctive combinatorial profiles of epigenetic modifiers. Our data reveal an unexpected and robust definition of cellular states by a cohort of epigenetic modifiers. Moreover, we determined the quantitative enrichment of specific chromatin modifiers in the ICM and asked whether they can be predictive of ICM determination. We find that one such modifier, *Prdm14*, shows a heterogeneous expression pattern in 4-cell-stage embryos and is subsequently highly enriched in ICM cells of the blastocyst. We show that expression of *Prdm14* at the 2-cell stage drives cells toward the pluripotent ICM. PRDM14 interacts with CARM1 and expression of *Prdm14* promotes H3R26me2. Our data underscore an instructive role for PRDM14 in regulating cell fate during early mammalian embryogenesis and suggest a model whereby PRDM14 and CARM1 function to promote pluripotency in vivo.

RESULTS

We performed a quantitative analysis of expression patterns in single cells using the Fluidigm Biomark System with 48:48 Dynamic Array chips coupled to TaqMan gene-expression assays. Single blastomeres were prepared by manual disaggregation of mouse embryos harvested at the required time points. We analyzed all embryo stages, from germinal-vesicle-stage oocyte to early blastocyst (3.5 days postfertilization), and included individual cells from both TE and ICM lineages. We analyzed the expression patterns of 39 genes and two internal controls (Table S1 available online). We focused our analysis primarily on enzymes that are involved in establishing or removing various histone lysine or arginine methylation marks. In addition, we included the DNA methyltransferases *Dnmt1*, *Dnmt3a*, *Dnmt3b*, and *Dnmt3l*, and four TFs that serve as ICM (*Nanog* and *Oct4*/*Pou5f1*) or TE (*Cdx2* and *Id2*) markers. This enabled us to correlate the expression patterns of chromatin modifiers to ICM and TE lineages and to validate the robustness of our data against that of a previous study that characterized expression of TFs in the mouse embryo (Guo et al., 2010; Figure S2). The absolute (unnormalized) levels of expression of all genes at all stages analyzed are shown in Figure S1. We validated a set of nine genes in single cells of the zygote and up to the 4-cell stage using quantitative RT-PCR (qRT-PCR), and at the protein level when antibodies were available (see below). Importantly, all genes analyzed behaved as predicted by the Biomark data in terms of both their average expression levels and their biological variability between individual cells of a particular stage (Figure S3).

Developmental Transitions Are Defined by Distinctive Combinatorial Profiles of Epigenetic Modifiers

We first addressed whether different developmental stages and degrees of cell potency can be defined on the basis of epigenetic components. For this purpose, we first performed unsupervised hierarchical clustering of all blastomeres and all genes (Figure 1A), which revealed that cells cluster primarily according to their developmental stage of origin, up to and including the majority of 8-cell-stage cells (Figure 1A). Thus, developmental phases can be defined by the expression of a cohort of chromatin modifiers. The oocyte, zygote, and 2-cell-stage blastomeres are clearly distinguished from the later stages of development, and therefore the maternal-to-zygotic transition

delineates the strongest difference in the clustering analysis. These earlier stages show strong expression of most of the chromatin modifiers analyzed, most likely reflecting the abundance of maternal transcripts present in oocytes and zygotes and, to a lesser extent, 2-cell-stage embryos (Hamatani et al., 2004). Interestingly, however, the oocyte and zygote do not express all genes and may also be characterized by the common absence or low expression of a number of genes, including *Suv39h1*, *Kdm4c*, and *Kdm5b*, whereas the *Dnmt1* transcript is specifically lost in zygotes. This is consistent with previous reports documenting loss of *Dnmt1* in zygotes while a differentially spliced isoform *Dnmt1o* is expressed (Ratnam et al., 2002). Note that the cells from the two lineages of the blastocyst, the ICM (E32I) and TE (E32O), cluster less well based on the chromatin modifiers they express compared with the TFs they express (compare Figures 1A and S2). Interestingly, ICM cells are more variable among themselves (Figure 1A, orange). This feature may reflect more flexibility or heterogeneity in ICM cells than in TE cells (see below).

Chromatin modifiers of similar activity do not seem to be coregulated, with a few exceptions. For example, the *Dnmt3a*, *Dnmt3b* de novo DNA methyltransferases and *Dnmt3l*, the noncatalytic DNA methyltransferase 3-like protein, all cluster in a group, suggesting that the de novo DNA methyltransferases share a common regulation across preimplantation development. This is probably required for the establishment of de novo DNA methylation patterns (Borgel et al., 2010; Okano et al., 1999). In addition, two histone H3K4 demethylases, *Kdm5a* and *Kdm5b* (formerly *Jarid1a* and *Jarid1b*), also consistently cluster together. Finally, the two PR-domain-containing proteins analyzed, PRDM14 and PRDM15 (of thus-far-unknown biochemical function) also cluster together, potentially reflecting similar or overlapping roles during early embryogenesis. Importantly, our data also uncovered variability in the gene-expression profiles of individual cells. For example, the Polycomb subunit *Ring1a* reproducibly shows high variability between cells at each stage (Figures 1A and S1).

Second, to investigate predominant gene-expression patterns, we applied principal component analysis (PCA) to our data set. This form of mathematical analysis identifies components of large gene-expression data sets that are able to reduce as much of the variance in the data set as possible into single dimensions, depicted on axes of a graph, highlighting similarities and differences within the data set. For the PCA shown in Figure 1B, the data points are the single cells taken from all stages of preimplantation development and the variables are the 39-dimensional gene set, normalized to the control genes. Each component in the PCA retains contributions from all the genes in the data set, and the relative contributions (weights) of the genes to each principal component are shown in Figure 1C, with genes with a more positive PC score enriched in cells with a more positive corresponding PC score. In the PCA of our gene-expression data set, the first component is represented on the x axis and explains 56% of the total variance in the data set. The second, uncorrelated component explains 5.6% of the remaining variance on the y axis.

The PCA reveals a striking distribution of all blastomeres according to their developmental origin, indicating that each developmental stage is characterized quantitatively and qualitatively by a precise combination of chromatin modifiers (Figure 1B). The first principal component (PC1, x axis) separates the cells into developmental stages ranging from oocyte to the 8-cell stage, indicating that the expression patterns of the chromatin modifiers differ sufficiently between stages to allow their segregation. The most significant variation in the data set is due to differences between early and later stages of development, with the 8-cell stage marking this transition (Figure 1B). Thus, this component does not simply reflect the maternal–zygotic transition, which is largely completed at the 2-cell stage. In contrast, from the 8-cell stage to the blastocyst stage, cells are no longer separated by PC1, but by PC2 on the y axis. The ICM (E32I) and TE (E32O) cells of the blastocyst are clearly distinct (defined in PC2), suggesting that the second most important variation in the data set is the segregation of the two lineages of the blastocyst. Only the 16-cell-stage blastomeres do not cluster into a developmental stage in the PCA, as they are spread between the positions of the ICM and TE cells of the blastocyst. This is likely to represent a gradient of chromatin modifier expression in the 16-cell-stage cells that reflects ICM and TE fates emerging from the subsequent round of development. Further, 2- and 4-cell-stage blastomeres are clearly distinguishable on the basis of the chromatin modifiers analyzed (Figure 1B), which may indicate that each stage has a distinct epigenetic status. Strikingly, 8-cell blastomeres are more similar to TE cells than to blastomeres at the nearest developmental time point, based on chromatin modifier expression (Figure 1B).

The PCA enables us to identify genes that are enriched at earlier stages of development, namely, *Suv39h2*, *Prmt2*, and *Kdm6b* (*Jmjd3*). For example, we find that *Prmt2* is a maternal transcript that is highly expressed in the oocyte and downregulated at fertilization up to the 16-cell stage. Zygotic expression of *Prmt2* presumably commences only at the blastocyst stage (Figure 1D). Importantly, this pattern of expression of *Prmt2* is recapitulated by the protein (Figure 1E). The mutually exclusive maternal expression of *Suv39h2* and zygotic expression of *Suv39h1* (Figures 1C, 1F, and 1G) is consistent with previous findings (Puschendorf et al., 2008). *Prdm14*, *Kdm4c* (*Jmjd2c*), *Kdm5b* (*Jarid1b*), and *Suv39h1* are genes with very low/absent transcripts in the oocyte and zygote, and their activation may therefore mark a developmental transition toward an embryonic chromatin configuration, concomitant with genome reprogramming (Figure 1A). *Kdm5a* (*Jarid1a*) appears as a strong contributor in demarcating the 8-cell stage (Figure 1C) and *Dnmt1* is on the extreme right-hand side of the PC1 component, suggesting that zygotic *Dnmt1* accumulation occurs at later stages of preimplantation development. This is in line with the known increase in zygotic Dnmt1 levels toward the blastocyst stage (Hirasawa et al., 2008).

Thus, early developmental transitions are marked by a distinctive pattern of epigenetic components, with the 8-cell stage marking the strongest transition in cellular states.

Earlier Developmental States Are More Clearly Demarcated by Chromatin Modifiers than Later States

To mathematically establish a time sequence in the development of individual cells, as well as the characteristics of their

Cell PRESS
Open ACCESS

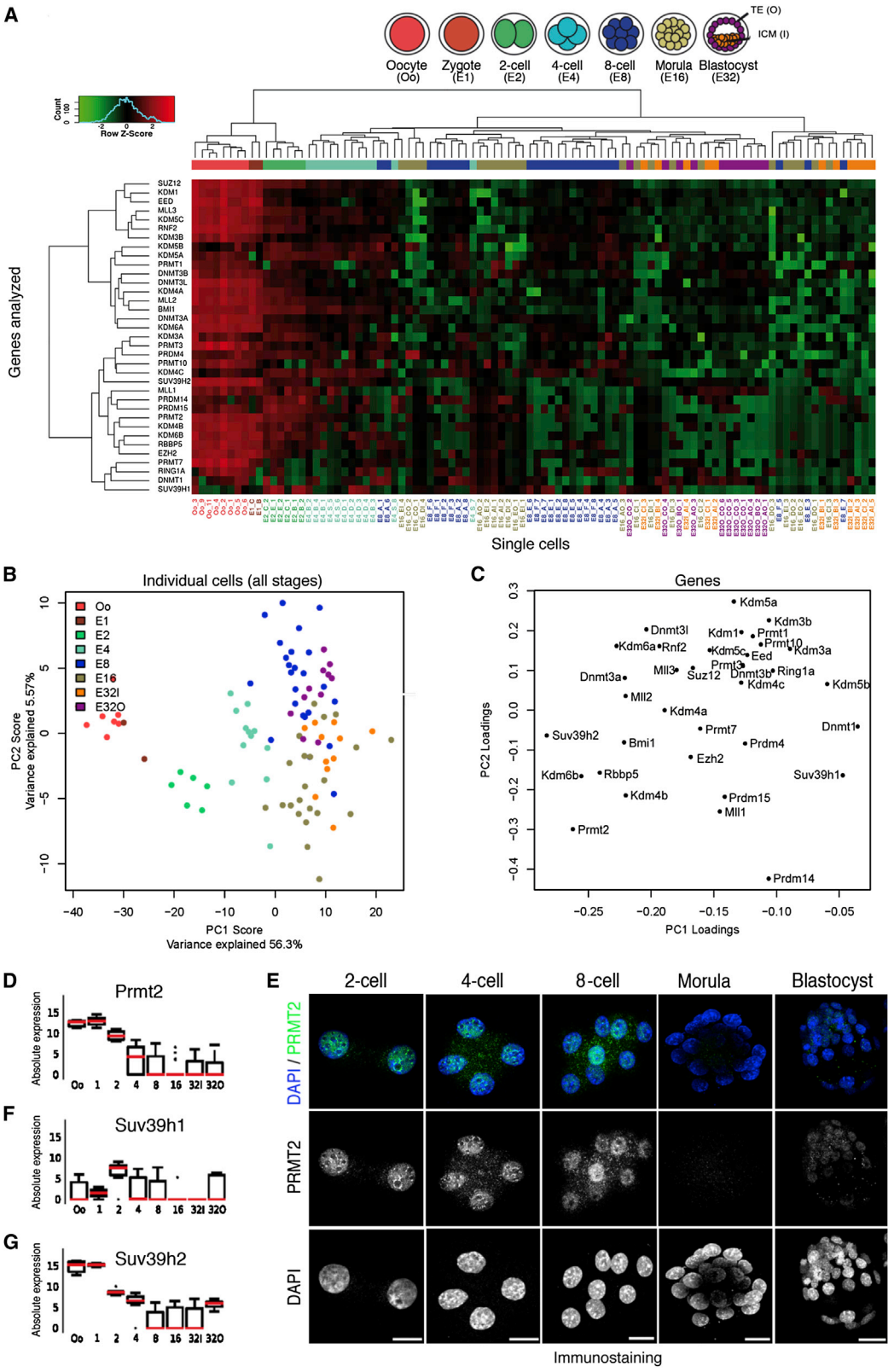

(legend on next page)

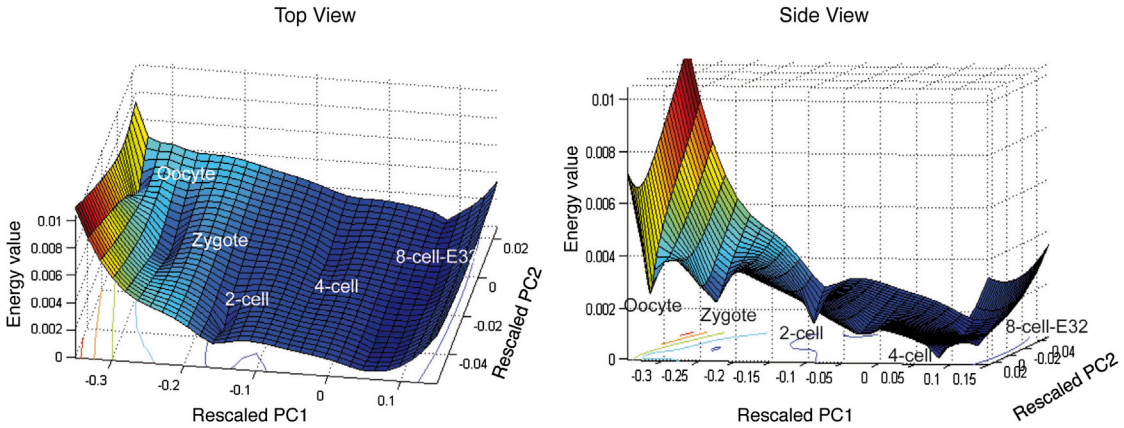

Figure 2. Epigenetic Landscape of Preimplantation Development Based on the Expression Profiles of Chromatin Modifiers

A semiquantitative epigenetic landscape was computed from the mean values (centers of gravity) and SDs (spread) of the individual cells for each developmental stage in the PCA in Figure 1B. The two panels represent top-down and side-on perspectives of the same landscape. The x and y axes correspond to the original PC1 and PC2 axes in the PCA of Figure 1B scaled by a factor of 0.01. The z axis refers to an energy value. The position (well) of each stage is indicated. The contours in the x and y axes represent the relative height of the landscape in the z axis (contour plots). From the 8-cell stage onward, the points in the PCA plane are grouped in a single cluster. Note that the distinction of the basins corresponding to stages later than 8-cell and to the ICM and TE on the epigenetic landscape is weaker compared with the much better defined cellular states for the stages between the oocyte and the 4-cell stage.

See also Figures S1, S4, and Table S1.

differentiation paths, we generated an epigenetic landscape based on the PCA in Figure 1B. For this purpose, we computed the center of gravity of each cluster of points (individual cells) in the PCA according to their position on the PCA plane (Figure S4). This mathematical analysis can be used to generate a probabilistic epigenetic landscape in analogy to the Waddington landscape (Bhattacharya et al., 2011. The computed, semiquantitative epigenetic landscape (Figure 2) has valleys ("creodes" according to Waddington's terminology) and some ridges. The valleys constitute stable steady states and the ridges can be interpreted as barriers to transitions between those cellular states. The landscape we generated from the PCA data reveals that there are only five clearly defined valleys, which correspond (from left to right) to oocyte, zygote (E1), 2-cell (E2), 4-cell (E4), and all 8-cell-blastocyst (E8–E32) stages together. It is clear and reasonable to assume that cells start near the oocyte "OO" valley and that the most likely transition to another well-defined differentiation state will correspond to the nearest point (in this case, the zygote [E1]) and subsequently to the 2-cell stage (E2). Likewise, from the 2-cell stage, the most probable transition is the 4-cell stage. In other words, a zygote will not develop into a 4-cell-stage "chromatin landscape," but will first transit through the 2-cell stage. However, there is no obvious transition from the 4-cell stage onward, as it is not clear which point is closest, and therefore this might reflect the fact that transitions from the 4-cell stage are not so well defined by the chromatin factors. In fact, we can observe that a definite proportion of the analyzed cells end up in distinct "differentiation" fates. Moreover, although the wells corresponding to oocyte, zygote, 2-cell, and 4-cell stages are well defined, those corresponding to the rest of the stages seem to merge into one larger well. The landscape also has a general downward trend from left to right (early to later), suggesting a directionality and that the "ball cannot go back," to use Waddington's analogy. This is particularly interesting because the transitions are consistent with the known time sequence of events (developmental progression).

Figure 1. Developmental Transitions Are Defined by Distinctive Combinatorial Profiles of Epigenetic Modifiers

(A) Hierarchical clustering of single cells derived from embryos at all stages, from oocyte to blastocyst, based on the expression levels of 35 chromatin modifiers with combined hierarchical clustering of chromatin modifiers. Each stage is colored according to the scheme above throughout the figures. Individual embryos are labeled with a letter (e.g., E8a) and individual blastomeres from each embryo are labeled with a number (e.g., E8a1-8). TE and ICM cells of the 32-cell-stage blastocyst were preidentified by labeling with a membrane dye. I, inner; O, outer.

(B) Principal component (PC) projection of individual cells based on the expression profiles of chromatin modifiers. The cells are colored according to embryonic stage as above. The first component represents the developmental transition from oocyte to the 8-cell stage on the x axis, and the second component represents ICM-to-TE lineage segregation on the y axis.

(C) PC projections of the 35 genes, showing the contribution of each gene to the first two PCs in Figure 1B. For example, a gene with a more positive PC2 loading is more enriched in cells with more positive PC2 scores in Figure 1B.

(D) Absolute unnormalized expression levels of *Prmt2* across preimplantation development. The boxed region represents the middle 50% of expression values, the black bar indicates the median values, and the whiskers indicate the maximum and minimum values. Cells with outlying expression values are depicted as dots.

(E) Expression of PRMT2 protein by immunofluorescence. Shown are maximum intensity projections of representative embryos. Scale bar is 20 μm.

(F and G) Absolute unnormalized expression levels of *Suv39h1* and *Suv39h2* as in Figure 1D.

See also Figures S1–S3 and Table S1.

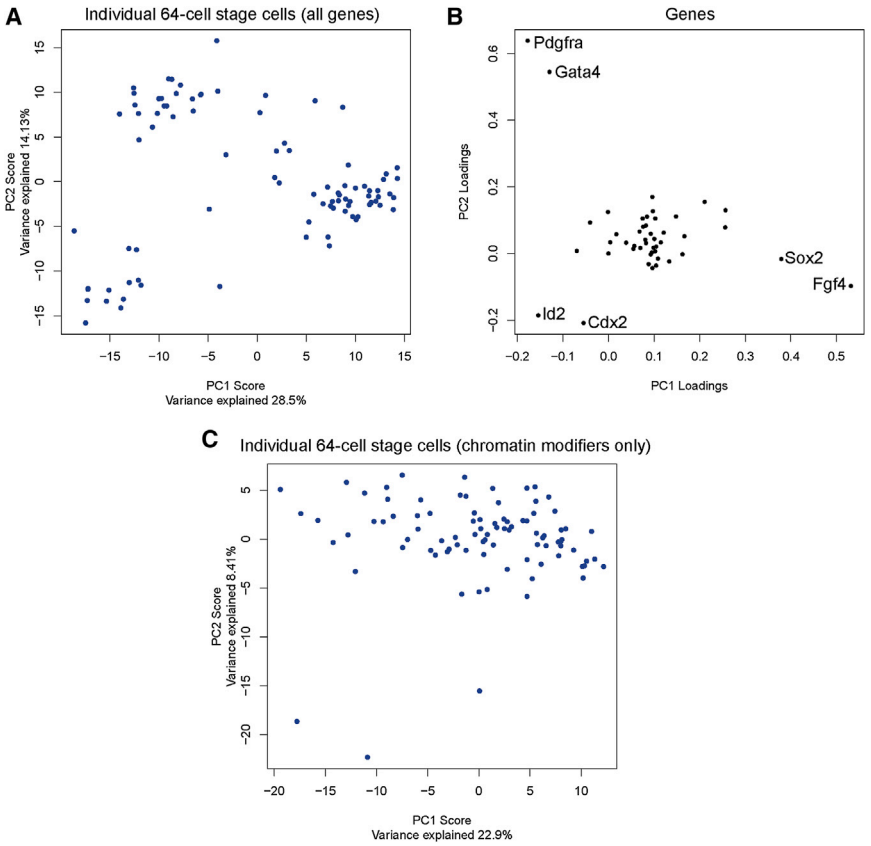

Figure 3. Late Developmental Transitions and Blastocyst Lineages Are Defined Better by TFs than by Chromatin Modifiers

(A) PC projections of 64-cell-stage blastocyst single blastomeres based on the expression levels of 37 chromatin modifiers and nine control genes. Each dot represents a single cell.

(B) Projections of the genes, showing the contribution of each gene to the first two PCs in (A). Note that the reference genes make each of the three clusters on the left panel identifiable as TE(*Id2*, *Cdx2*), EPI (*Sox2*, *Fgf4*), and PE (*Gata4*, *PdgfrA*).

(C) PC projection of individual cells of 64-cell-stage embryos based on the expression profiles of the 37 chromatin modifiers analyzed in (A). Note that the different lineages are no longer distinguishable in the absence of reference TF and signaling genes.

See also Figure S1and Tables S1 and S2.

The temporal sequence in this model originates from the differences in the expression of chromatin modifiers and shows that the earliest stages are better defined than the later stages based on their chromatin constituents. This finding contrasts with results obtained from single-cell expression data for TFs and signaling proteins, which show that there are no significant variations between single cells prior to compaction, and instead define clear developmental transitions and lineage segregation at later stages of development (Guo et al., 2010). To address this distinction in more detail, we generated single-cell expression data from 64-cell-stage embryos to profile 37 chromatin modifiers and nine control and reference genes (*Pou5f*, *Nanog*, *Sox2*, *Fgf4*, *Pdgfra*, *Gata4*, *Cdx2*, *Id2*, and *Actin-B*; Table S2). Because we included these relevant marker genes of the three lineages of the late blastocyst (EPI, PE, and TE) in this analysis, and the number of genes that one can analyze in the Biomark is limited, the list of genes analyzed in this experiment is not identical to that shown in Figure 1 (Table S2). Nevertheless, PCA with 37 chromatin modifiers and nine reference genes shows that three lineages can be clearly distinguished in 64-cell-stage embryos, with three clusters of groups of cells (Figure 3A). These clusters correspond to the three lineages of the 64-cell-stage blastocyst (the EPI, PE, and TE), as can be appreciated from the loading position of the respective marker genes on the PCA (*Cdx2* and *Id2* for the TE, *Gata4* and *PdgfrA* for the PE, and *Fgf4* and *Sox2* for the EPI; Figure 3B). In contrast, when we performed the PCA with only the 37 chromatin modifiers, we observed no clear resolution of lineages, and instead the same cells were distributed in a scatter along the principal components (Figure 3C). Thus, our data indicate that the three lineages of the 64-cell-stage embryo cannot be distinguished on the basis of the chromatin modifiers they express. This lends support to our hypothesis that chromatin modifiers define early developmental transitions better than at later stages, when lineages can be resolved based on the expression of specific transcription and signaling factors.

Nonbiased Analysis of Epigenetic Modifiers Delineates Cellular Differentiation States

We next addressed in detail the unexpected similarity between the 8-cell-stage and TE cells of the blastocyst with regard to the expression profiles of their chromatin modifiers. Importantly, this similarity is lost if TFs are included in the data set (data not shown), demonstrating that the similarity between these two cell types is reflected more by chromatin modifiers than TFs, most likely due to the dramatic upregulation of *Cdx2* and *Id2* in the TE. First, we analyzed further the potential similarity between the 8-cell-stage and TE cells by performing a PCA of just the later stages of development (4-cell to 32-cell stages; Figure 4A). We found that the 8-cell-stage blastomeres reproducibly segregate together with the TE cells. Second, to identify the chromatin modifiers that are more strongly expressed in these two stages, as opposed to the ICM cells, we analyzed the raw expression data. This revealed three genes with similar expression in 8-cell blastomeres and TE cells, but not in ICM cells (Table S3). These included the H3K4me2/3 demethylase *Kdm5a*/*Jarid1a*, the H3K27me2/3 demethylase *Kdm6a*/*Utx*, and *Dnmt3l*, which were all similarly more strongly expressed in 8-cell-stage and TE cells compared with ICM cells (Figure 4B). We validated this enrichment pattern for one of these three proteins, KDM5A/JARID1A. Indeed, the nuclear accumulation of KDM5A/JARID1A

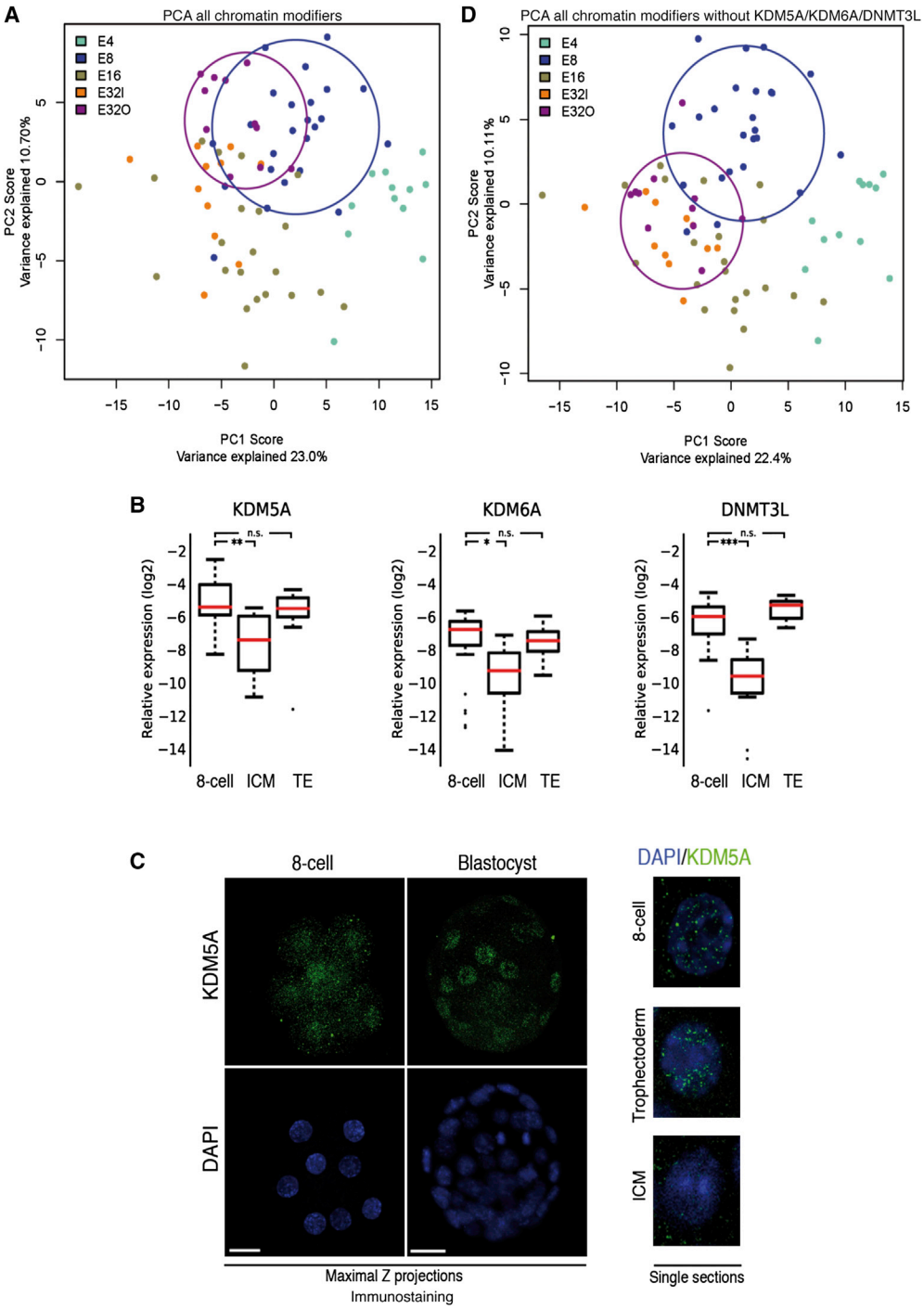

Figure 4. Similarity between 8-Cell-Stage and TE Cells, Defined by Three Chromatin Modifiers

(A) PC projections of 4-cell-stage to blastocyst single blastomeres based on the expression levels of 35 chromatin modifiers. Each dot represents a single cell. Colored rings indicate the relative positions of the 8-cell-stage and TE cells in blue and purple, respectively.

(B) Relative expression levels of the indicated genes in 8-cell-stage, ICM, and TE cells. *$p < 0.01$, **$p < 0.001$, ***$p < 0.0001$ (Mann-Whitney test).

(C) Analysis of KDM5A protein in 8-cell-stage cells and blastocysts by immunofluorescence. A single section merge of representative 8-cell stage, TE, and ICM nuclei is shown on the right. Scale bar is 20 μm.

(D) PC projections of 4-cell-stage to blastocyst single cells based on the expression levels of chromatin modifiers except for *Kdm5a*, *Kdm6a*, and *Dnmt3l*. The relative positions of 8-cell-stage and TE cells are indicated by blue and purple circles, respectively. Note that the 8-cell-stage cells and TE cells are now well separated.

See also Figure S1 and Tables S1 and S3.

was lower in the ICM than in the TE and 8-cell-stage blastomeres (Figure 4C). Importantly, when we removed these three genes from the data set before repeating the same PCA as shown in Figure 4A, we observed that the 8-cell-stage and TE cells failed to cluster together, indicating that the expression profiles of these three genes define the similarity between these stages (Figure 4D).

During both of these stages of development, these two types of cells uniquely undergo a differentiative transition. At the 8-cell stage, the first overt changes occur in the embryo as the individual cells develop polarity, enabling subsequent differentiative cell divisions (Ziomek and Johnson, 1980). Similarly, TE cells of the blastocyst are also in the process of differentiating, accompanied by polarization and epithelization (Rossant and Tam, 2009). Therefore, we hypothesize that the similar pattern of expression of chromatin modifiers in these two cell types might result in a similar chromatin architecture that could be permissive for differentiation. Our data suggest that JARID1A, UTX, and DNMT3L may play important roles in setting up a chromatin configuration necessary for establishing and/or maintaining the processes of polarization that occur during these two stages of development.

The Two Lineages of the Blastocyst Can Be Segregated According to Distinct Profiles of Chromatin Modifiers

The blastocyst is composed of two lineages with very different states of potency: the TE, which is the first differentiated tissue in the embryo and therefore has a limited capacity to further differentiate, and the ICM, which is pluripotent and the origin of embryonic stem cells (ESCs). We thus asked whether these two distinct cell types are defined by different combinations of chromatin modifiers. We analyzed these two lineages in isolation. First, we performed PCA and unsupervised hierarchical clustering of the individual blastomeres derived from TE or ICM lineages with the chromatin modifiers and the TF data (Figures 5A and S5A). This analysis resulted in segregation into two well-defined groups containing either ICM (E32I) or TE (E32O) cells ($p < 0.002$; Figures 5A and S5A). The TFs *Cdx2* and *Id2* clustered together, with higher expression in the TE cells as expected (Figure S5A). The TF factors characteristic of the ICM *Oct4* and *Nanog* were not so obviously enriched in the ICM cells at this stage (Figures 5B and 5C). This could reflect the greater heterogeneity in the ICM cells, which do not cluster as well as the TE cells, supporting the view that the TE cells are defined earlier than the ICM and that the markers for the ICM are not completely segregated until one or two cycles later (Dietrich and Hiiragi, 2007).

To determine whether ICM and TE cells can be identified based on the repertoire of chromatin modifiers they express, we performed an analysis of all blastocyst cells, but in the absence of the TF data set. Importantly, this also resulted in the segregation of ICM and TE ($p < 0.025$; Figures 5D and S5B). This reveals that ICM and TE cells at this stage of development possess mostly distinct expression patterns of chromatin modifiers. The ICM versus TE segregation is still the most significant distinction within the data set in the first principal component, although the proportion of the variance in the data set explained by this component is significantly higher in the presence of the TFs (Figure 5A).

We next sought to identify chromatin modifiers that would impose a signature on either lineage. Figure 5E reveals the chromatin modifiers that make the greatest contribution to the segregation of ICM versus TE. Notably, *Prdm14* is the most enriched gene in ICM cells. Conversely, *Dnmt3l* and *Dnmt3b* are the most enriched chromatin modifiers in TE cells and, to a lesser extent, the H3K9 methyltransferase *Suv39h2* (Figure 5E). Ordering individual cells according to their first PC score (Figure 5F), and plotting the expression levels of the selected genes accordingly, further revealed very similar behavior of *Dnmt3b* and *Dnmt3l*, with high expression in TE cells gradually decreasing to lower levels in ICM cells (Figure 5F). *Prdm14*, on the other hand, is only expressed in two cells of the TE, and then at low levels, whereas its expression is higher but heterogeneous in ICM cells (Figure 5F). We validated the *Prdm14* and *Dnmt3l* patterns of expression in the blastocyst stage by an independent approach using single-cell qRT-PCR without preamplification (Figure S5C). Importantly, a previous reporter construct showed enriched expression of *Prdm14* in the ICM (Yamaji et al., 2008), and we confirmed the mRNA pattern of DNMT3B at the protein level, which appears largely enriched in the TE (Figure 5G; see also Hirasawa and Sasaki, 2009). To identify whether these chromatin modifiers show differential expression levels across individual cells of the 32-cell-stage blastocyst, we generated violin plots (Figure S5D). The TE markers show a clear bimodal expression, reflecting strong expression levels in some cells (TE cells) and very low or no expression in other cells (ICM cells). The ICM markers, however, do not show a bimodal distribution, supporting earlier observations (Dietrich and Hiiragi, 2007; Figure 5C). Notably, *Prdm14* adopts the most extreme distribution of the genes analyzed, farther to the right than *Nanog* or *Oct4* in the PCA shown in Figure 5B. In line with this, *Prdm14* shows a bimodal expression (Figure S5D; data not shown), whereas *Dnmt3b* and *Dnmt3l* exhibit a more graded expression pattern, fitting with their profiles in Figure 5F.

Thus, the two lineages of the blastocyst can be identified by the combination of chromatin modifiers that they express, and the ICM cells show greater heterogeneity in this respect. In particular, *Dnmt3b* and *Dnmt3l* are enriched in TE cells, whereas *Prdm14* is highly enriched in a subpopulation of the ICM.

PRDM14 Is Asymmetrically Distributed in 4-Cell-Stage Blastomeres

In light of the importance of uncovering the molecular mechanisms that regulate the formation of pluripotent cells, we next wondered whether we could identify chromatin modifiers that might play an early, instructive role in ICM cell-fate allocation. Our observation that *Prdm14* is more enriched in ICM cells than *Nanog* and *Oct4* (Figure 5B) prompted us to ask whether PRDM14 could play a role in lineage allocation at an earlier stage. PRDM14 is a PR-domain and zinc finger (ZF) protein whose expression is restricted to early embryonic tissues during periods of cellular reprogramming and is required for establishment of germ cells and maintenance of the ESC ground state (Gillich et al., 2012; Ma et al., 2011; Yamaji et al., 2008, 2013). PRDM14 is a sequence-specific regulator of gene expression

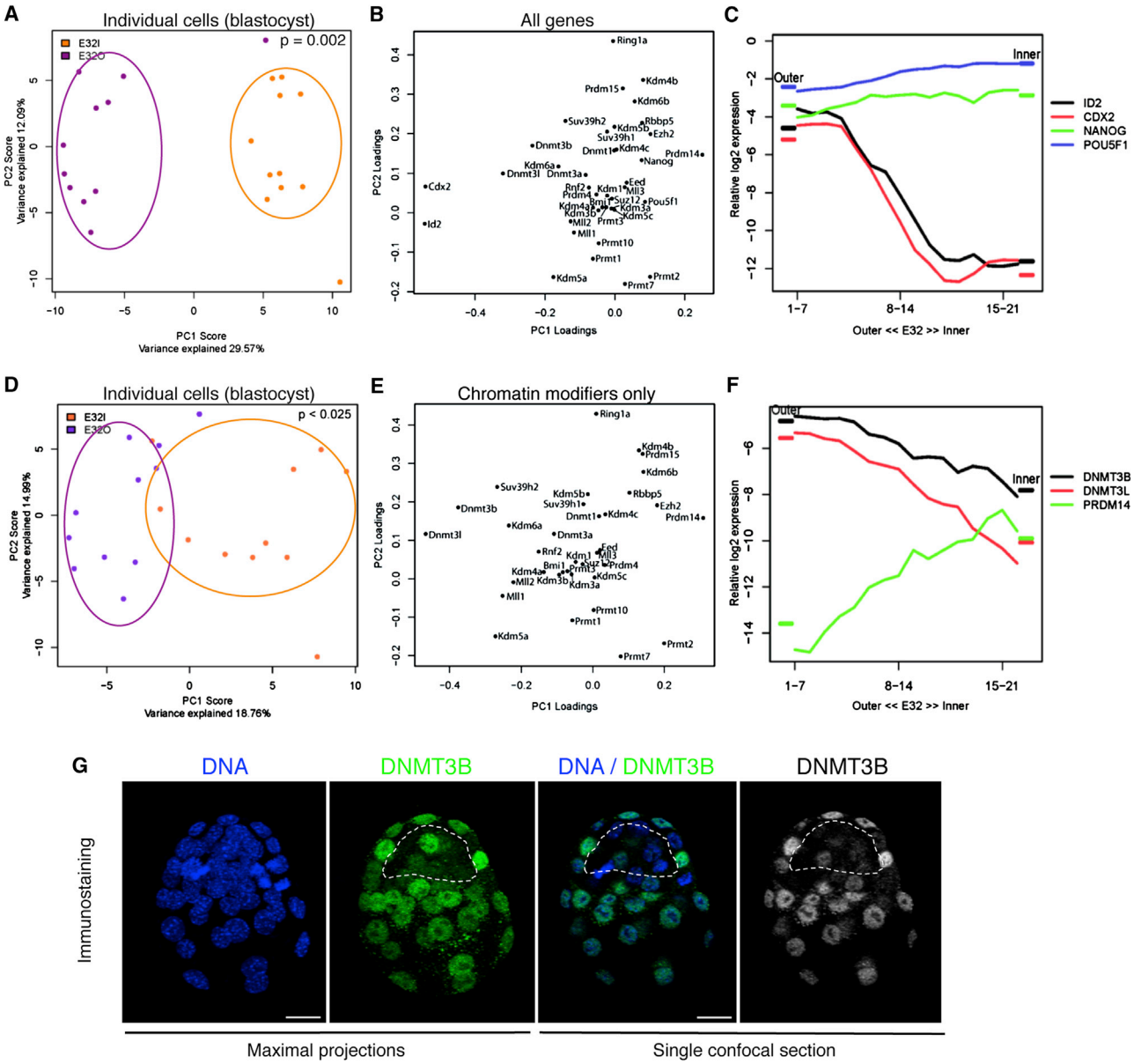

Figure 5. The Two Lineages of the Blastocyst Can Be Segregated According to the Distinct Profiles of Chromatin Modifiers

(A) PC projection of individual cells from early blastocysts based on the expression of chromatin modifiers and TFs. The calculated probability of equality between ICM (E32I) and TE (E32O) is indicated (Kolmogorov-Smirnov test). The orange and purple circles visually indicate the relative positions of ICM and TE cells, respectively.

(B) PC projections of the 39 genes (chromatin modifiers and TFs), showing the contribution of each gene to the first two PCs in (A). The ICM and TE TF "markers" are on the extremes of the PC1, enriched with the positions of the ICM and TE cells in (A), strongly suggesting that this most significant component distinguishes ICM from TE cells.

(C) Expression profiles of TFs characteristic of the ICM and TE across the population of single cells in the blastocyst. Blastomeres were ordered along the x axis according to the PC1 score in (A). The traces represent the average normalized expression value of each in gene in moving windows of seven cells. The colored bars labeled "Outer" and "Inner" represent the mean expression levels at the blastocyst stage for TE and ICM, respectively.

(D) PC projection of individual cells from early blastocysts based on the expression of chromatin modifiers alone, showing a clear segregation of ICM and TE cells in the PC1. The calculated probability of equality between ICM and TE groups is indicated (Kolmogorov-Smirnov test). The orange and purple circles visually indicate the relative positions of ICM and TE cells, respectively.

(E) PC projections of the 35 chromatin modifier genes, showing the contribution of each gene to the PCA in (D).

(F) Expression profile of *Prdm14*, *Dnmt3b*, and *Dnmt3l* in the blastocyst across the population of single blastomeres. Blastomeres were ordered along the x axis according to the PC1 score in (D). The traces represent the average normalized expression value of each gene in moving windows of seven cells.

(G) Immunostaining of DNMT3B at the early blastocyst stage confirms enrichment in TE relative to ICM. Maximal Z projection and a single confocal section for a representative blastocyst are shown. The position of the ICM is depicted by a dotted line. Scale bar is 20 μm.

See also Figures S1, S5 and Table S1.

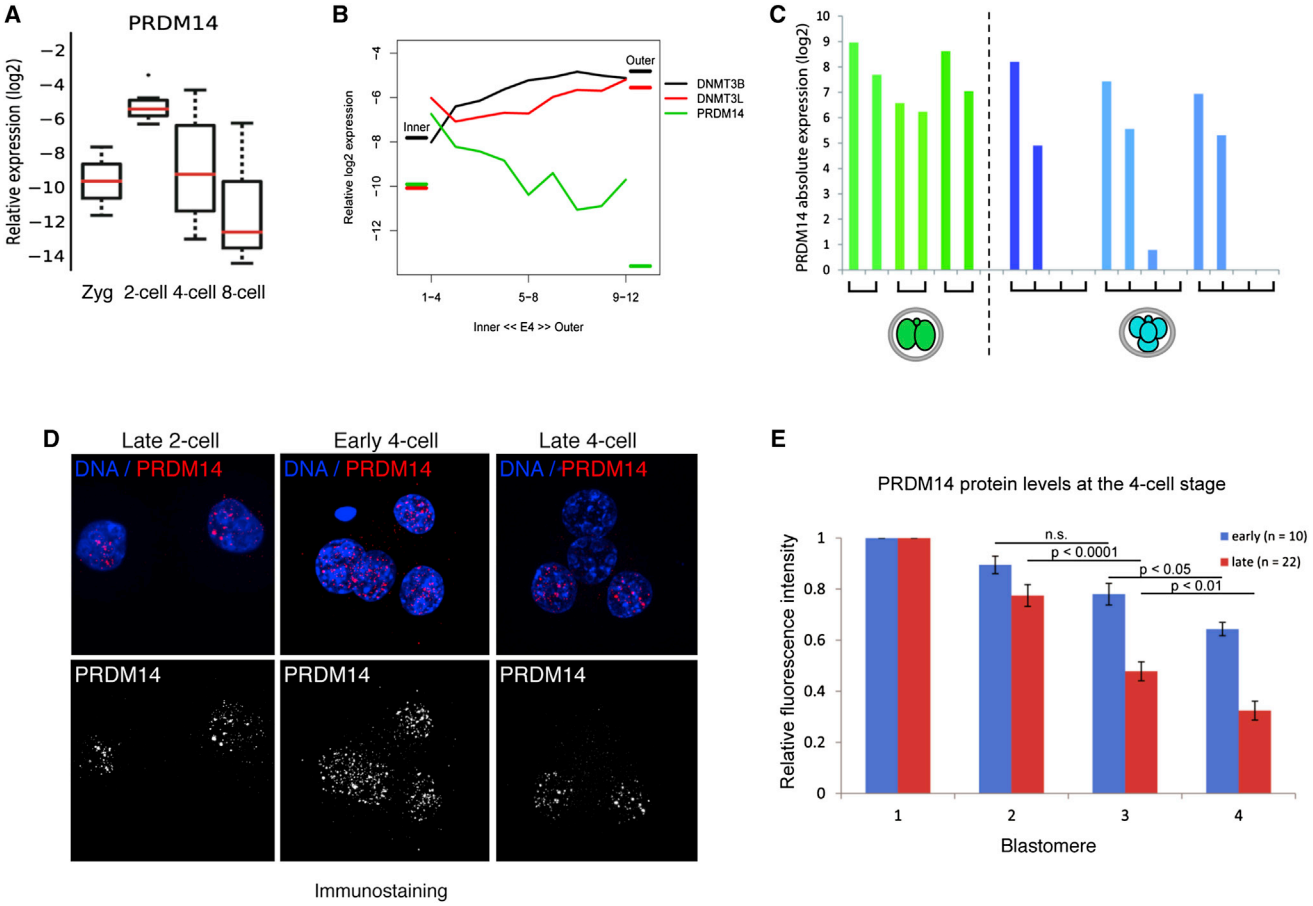

Figure 6. PRDM14 Expression Is Heterogeneous at the 4-Cell Stage

(A) Average expression levels of *Prdm14* normalized to control genes between the zygote and the 8-cell stage.

(B) Expression levels of *Prdm14*, *Dnmt3b*, and *Dnmt3l* across the 4-cell population. Single cells were ordered along the x axis based on the PC1 scores of a PCA of 4-cell-stage cells. The average normalized expression value of each gene in moving windows of four cells was then plotted (as for Figure 5C). A gradient of *Prdm14* expression is observed that inversely correlates with expression of *Dnmt3b* and, to a lesser extent, *Dnmt3l*. The colored bars labeled "Outer" and "Inner" represent the mean expression levels at the blastocyst stage for TE and ICM, respectively.

(C) Bars represent the absolute, unnormalized *Prdm14* expression level in each cell of three 2-cell (green) and three 4-cell (blue) stage embryos.

(D) Immunofluorescence of PRDM14 in late 2-cell and early and late 4-cell-stage embryos. Shown are maximum intensity projections of representative embryos. Scale bar is 20 μm.

(E) Quantification of PRDM14 in early and late 4-cell-stage embryos. The fluorescence intensity per nucleus was normalized to the nucleus with the strongest staining per individual 4-cell-stage embryo, and the mean averages of these ratios are shown (± SEM). The Mann-Whitney U test was applied.

See also Figures S1 and S6, Table S1.

that plays both activating and repressive roles in transcription depending on the chromosomal context. Interestingly, we find that, unlike the lineage-specific TFs, which function in lineage allocation at later stages, *Prdm14* is strongly expressed at the 2-cell stage; its expression is downregulated and becomes highly variable at the 4- and 8-cell stages, and is subsequently lost by the 16-cell stage (Figure 6A). Ordering of 4-cell-stage blastomeres according to the first principal component scores of the PCA based on just the single 4-cell-stage blastomeres (not shown) reveals a gradient of *Prdm14* expression, indicating that *Prdm14* shows strong variations in its expression levels among individual 4-cell blastomeres (Figure 6B). Interestingly, we find opposing patterns of expression of *Dnmt3b* and *Dnmt3l* compared with that of *Prdm14* at the 4-cell stage (Figure 6B), similarly to the inverse correlation found in the blastocyst. Expression of *Prdm14* at the 4-cell stage is weakly correlated with *Oct4* (R = 0.56) and *Nanog* (R = 0.42), whereas the outer markers are very weakly or not expressed at this stage. Importantly, analysis of single cells from individual embryos revealed that heterogeneous *Prdm14* expression emerges at the 4-cell stage and is strikingly intraembryonic, with two blastomeres of each 4-cell-stage embryo expressing *Prdm14* and the other two showing no or very low *Prdm14* expression (Figure 6C). We next addressed whether the asymmetric distribution of *Prdm14* mRNA levels translates into changes in accumulation of the protein between blastomeres. Remarkably, we find that although 2-cell-stage and early 4-cell-stage blastomeres display equivalent levels of PRDM14 protein, late 4-cell-stage embryos

display an asymmetric distribution of PRDM14, with two cells displaying strong nuclear accumulation of PRDM14 and two cells showing low levels, in agreement with the mRNA pattern (Figures 6D and 6E). Thus, PRDM14 is heterogeneously distributed in late 4-cell embryos, suggesting that epigenetic differences develop by the end of the 4-cell stage.

PRDM14 Promotes H3R26 Methylation and Directs Cells toward the Pluripotent ICM

Given the opposing patterns of expression of *Prdm14* versus *Dnmt3b/3l* in the blastocyst, the high enrichment of *Prdm14* in the ICM, and the remarkable asymmetry of its accumulation at the 4-cell stage, we hypothesized that PRDM14 may play a role in lineage allocation, with cells expressing higher levels of *Prdm14* being more likely to generate ICM cells. To test this hypothesis directly, we overexpressed PRDM14 by injecting its mRNA in combination with that of GFP as lineage tracer into one cell of a late 2-cell-stage embryo and monitored development to the blastocyst (Figure 7A). We verified that injection of mRNA for PRDM14 resulted in elevated levels of the protein at the 4-cell stage (Figures 7B and S6A). Embryos overexpressing *Prdm14* developed normally and reached the blastocyst stage in ratios similar to those observed for embryos injected with mRNA for GFP only (summary: Table S4; raw data: Tables S5 and S6). We reconstructed the resulting blastocysts in three dimensions as described previously (Torres-Padilla et al., 2007) using cortical F-actin staining to locate every inner (ICM) and outer (TE) cell in the blastocyst to determine which lineage the labeled cells had contributed to (Table S4; Movies S1 and S2). The blastocyst at this stage is composed mostly of TE cells (approximately two-thirds of the total cells are TE cells). In control embryos, therefore, the expected random contribution to the ICM of a 2-cell blastomere progeny is one-third, which accurately corresponds to the one we obtained upon injection of GFP only (30.97% ± 7.38%; Tables S4 and S5; Movie S1). In contrast, we consistently observed a higher than expected contribution to the ICM of the progeny of the *Prdm14*-injected cell ($p = 0.0058$; Figure 7C). The proportion of the *Prdm14*-clone allocated to the ICM was 1.37-fold higher than that of the control *Gfp*-clone: 41% for *Prdm14* versus 30% for a random, GFP distribution (Tables S4–S6; Movies S2 and S2). Representative control and *Prdm14*-injected blastocysts are shown in Figure 7D.

In order to dissect the requirement of the functional domains within PRDM14 for cell-fate induction, we generated three different constructs: (1) PRDM14 lacking the ZF and therefore unable to bind to DNA (Ma et al., 2011), (2) PRDM14 lacking the PR domain, and (3) PRDM14 lacking the N terminus and containing only the PR and ZF domains (Figure 7E). The PR-ZF-only PRDM14 construct did not localize in the nucleus and instead resulted in cytoplasmic accumulation of PRDM14, precluding further analysis (data not shown). Importantly, expression of the PRDM14ΔZF construct did not cause an effect on cell fate, suggesting that DNA binding is required for induction of ICM cell fate (Figure 7C; Tables S4 and S7). Expression of PRDM14ΔPR in individual 2-cell blastomeres resulted in two distinct phenotypes. A large majority of the embryos (78%; $n = 22$) developed abnormally. Either these embryos did not generate a correct number of cells in the blastocyst or the contribution of the Prdm14ΔPR-injected cells to the total number of cells was less than 50%, suggesting a potential dominant-negative effect with a deleterious impact on development or cell division. In the remaining 22% of the embryos that reached the blastocyst stage, expression of PRDM14ΔPR did not result in a consistent effect on cell-fate allocation (Table S8). Thus, we conclude that overexpression of *Prdm14* in a 2-cell blastomere leads to a biased contribution of that cell to the ICM in the blastocyst, and that both the ZF and the PR domain of PRDM14 are required for this effect.

The only other protein known to date to affect cell-fate allocation during preimplantation development is CARM1/PRMT4, whose overexpression also directs cells toward the ICM (Torres-Padilla et al., 2007). Therefore, we next asked whether PRDM14 and CARM1 might function in the same pathway. Unfortunately, we had to omit *Carm1* from our Fluidigm analyses because the Taqman assays available did not produce a reliable quality control. To determine whether PRDM14 and CARM1 function in parallel, we first examined whether PRDM14 affects global levels of H3R26 methylation, a substrate of CARM1 (Chen et al., 1999). Expression of *Prdm14* in one 2-cell blastomere led to a significant 1.5-fold increase in global H3R26me2 levels compared with noninjected or GFP-only-injected controls (Figures 7F and S7), similar to *Carm1* overexpression (Torres-Padilla et al., 2007). In line with the cell-fate effects described above, neither the PRDM14ΔZF nor the PRDM14ΔPR constructs affected H326me2 levels (Figures 7F and S7). Second, we asked whether PRDM14 and CARM1 physically interact, which would provide a mechanistic basis for PRDM14 and CARM1's function in cell-fate allocation. We performed coimmunoprecipitation analyses in ESCs because they express both proteins endogenously (Figure 7G), and because we cannot perform immunoprecipitation in embryos due to the limited amount of material they can provide. We used 3T3 fibroblasts as a negative control because they do not express PRDM14 (Figure 7G; Yamaji et al., 2008). We find that endogenous CARM1 coimmunoprecipitates with PRDM14, suggesting that both proteins act together on some of their targets to regulate chromatin function.

DISCUSSION

The period of preimplantation development results in the generation of a differentiated blastocyst capable of implantation. This differentiation is accompanied by a transition from totipotency to the allocation of two distinct lineages with two distinct cellular potency states: pluripotent and differentiated. Our study provides insights into the quantitative and combinatorial expression patterns of 35 key chromatin-modifying enzymes during these dynamic shifts in the cellular state, at single-cell resolution.

Approaches that address single-cell dynamics are becoming crucial to understand both the significance of biological heterogeneity and the molecular changes that occur upon defined cell-fate transitions. This will be essential for elucidating complex biological processes and obtaining single-cell measurements with high temporal and spatial resolution. This in turn will allow the generation of kinetic models that can be used to predict regulators and their mode of action. Earlier microarray studies with

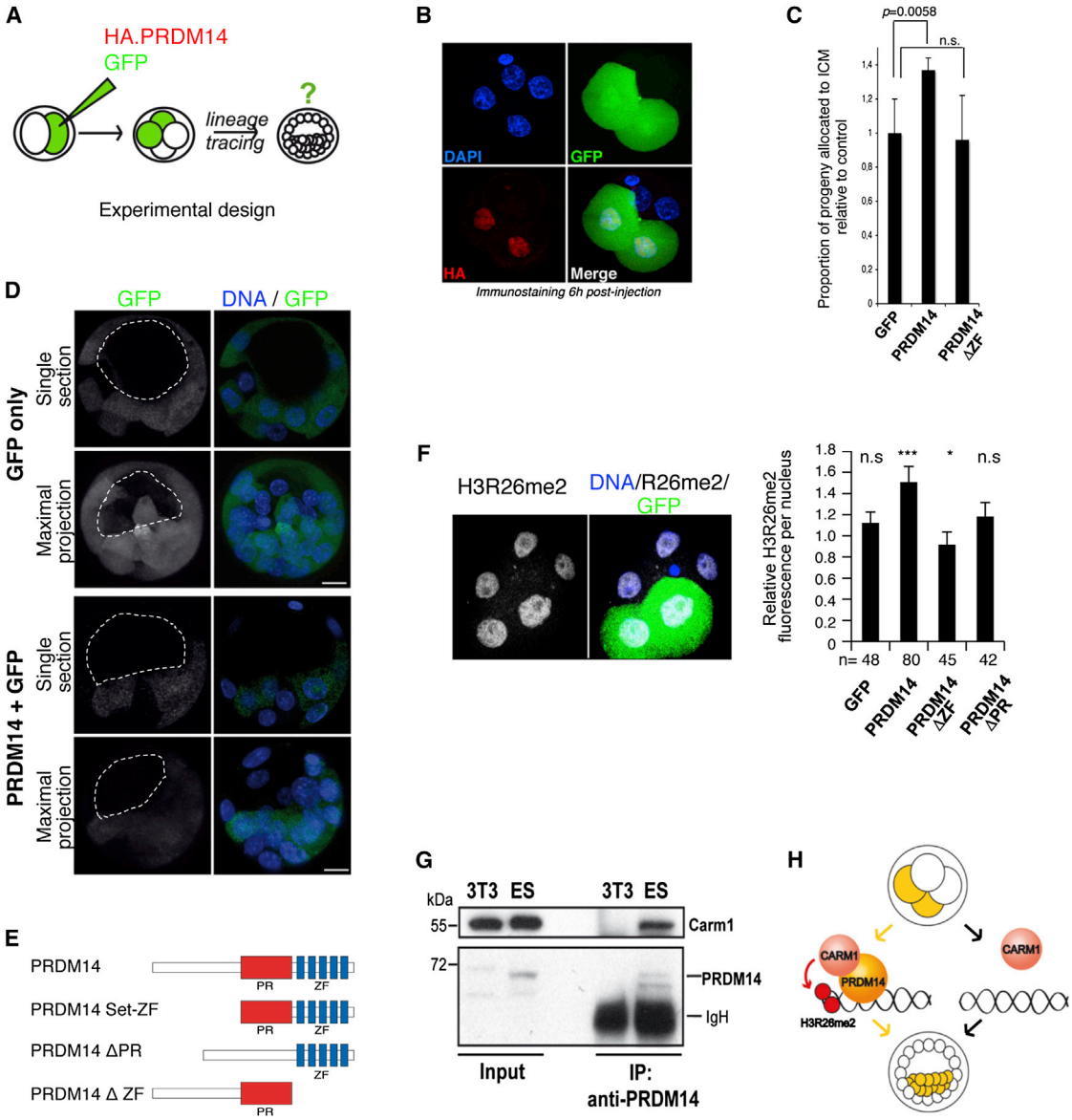

Figure 7. PRDM14 Directs Cells toward the ICM from the 4-Cell Stage

(A) Outline of the experimental design. A single 2-cell blastomere was microinjected with *HA-Prdm14* and *gfp* or *gfp* mRNA alone. Embryos were cultured until the blastocyst stage and then fixed. The GFP-positive progeny of the injected cell were then positioned as inner or outer cells by 3D digital image reconstruction.

(B) Embryos injected as above and stained with HA antibody. Shown is a maximum intensity projection of a representative embryo. Scale bar is 20 μm.

(C) *Prdm14* expression biases cells toward an ICM fate. The proportion of the progeny of the PRDM14-injected and PRDM14ΔZF-injected cells allocated to the ICM is shown relative to the GFP controls, which was set at one and corresponds to the expected random contribution (the raw data are shown in Tables S4–S7).

(D) Representative blastocysts from the PRDM14- and GFP-injected groups. The position of the cavity is indicated with a dashed line. Scale bar is 20 μm.

(E) Schematic of PRDM14 and the deletion constructs used, indicating the PR domain (aa 241–362) and the C-terminal domain containing six ZFs (aa 390–561).

(F) PRDM14 microinjection leads to increased H3R26me2 levels. Embryos were injected as in (A), fixed 24 hr later, and stained with an H3R26me2 antibody. Shown is a maximum intensity projection of a representative embryo. Scale bar is 10 μm. The graph shows the average of the ratio of fluorescence intensity (± SEM) of the H3R26me2 signal per nucleus in GFP-only and PRDM14-, PRDM14ΔZF-, and PRDM14ΔPR-injected progeny nuclei compared with noninjected progeny nuclei per embryo. The Mann-Whitney U test was applied.

(G) PRDM14 interacts with CARM1 in ESCs. Mouse ESCs or 3T3 cells were subjected to immunoprecipitation with a PRDM14 antibody. Membranes were probed with a CARM1 or PRDM14 antibody as control.

(H) Working model depicting the proposed mechanism for the cooperative role played by PRDM14 and CARM1 in biasing cell fate toward the ICM lineage. PRDM14 associates with CARM1 and targets this histone methyltransferase to chromatin via the ZF DNA-binding domain of PRDM14. At the late 4-cell stage, the two cells that express higher levels of PRDM14 thus have more chromatin-associated CARM1, resulting in globally higher levels of histone arginine methylation (e.g., H3R26me2), which in turn leads to transcriptional activation of the genetic program for establishing the ICM lineage.

See also Figures S1, S6, and S7, and Tables S1 and S4–S8, and Movies S1 and S2.

whole embryos or RNA sequencing in single cells (Hamatani et al., 2004; Wang et al., 2004; Tang et al., 2011) shed light on the global changes that accompany developmental progression. In contrast to our analysis, which used total RNA, those studies were performed using polyadenylated mRNA. We used total RNA because of the known regulation of mRNA translation in the embryo due to the absence of polyA or the use of alternative polyA lengths, and therefore this should be taken into account for future and comparative analyses. Moreover, the use of microfluidics technology combined with gene-specific Taqman assays reduces the amplification bias, which represents a major advantage when addressing quantitative parameters in single cells (Guo et al., 2010; Lorthongpanich et al., 2012).

The computed epigenetic landscape we generated highlights that the expression patterns in the oocyte, zygote, and 2- and 4-cell-stage cells are more different from each other than those observed in later stages, and that the most dramatic changes in expression of chromatin modifiers take place at earlier stages. This could imply that the most dramatic "epigenetic reprogramming" occurs earlier. Later on, there are more subtle differences, suggesting that only a few chromatin modifiers define later transitions (e.g., PRDM14/DNMT3L for ICM versus TE cells). Alternatively, it could be that at later stages of development, the "control" of cell fate is no longer epigenetic, but rather occurs via TFs, raising the possibility that the chromatin first sets up an environment for cell-fate "choices" and subsequently the TFs consolidate those choices. It should be noted that although most chromatin modifiers do not show a preimplantation phenotype when knocked out, the function of these genes during early development has not been examined because many of them are inherited maternally. Indeed, in the few cases in which chromatin modifiers were deleted in the maternal germline, such as for Ezh2 and Brg1, an early preimplantation phenotype was observed (Bultman et al., 2006; Erhardt et al., 2003). Our study highlights the need to perform maternal knockout studies on specific chromatin modifiers to determine whether they may play a role in reprogramming.

Based on the signature of chromatin modifiers, individual cells segregate into their embryonic stage rather than individual embryos. This suggests that significant transitions occur in the composition of chromatin modifiers between stages over the course of preimplantation development, which is likely to be reflected by a dynamically evolving chromatin architecture during this period. We therefore hypothesize that chromatin-based changes that accompany the transitions in potency and lineage allocation are functionally important for these processes. Indeed, we validated this hypothesis by demonstrating a role for PRDM14 in inducing lineage allocation from the 4-cell stage. The PRDM family of proteins is best characterized by PRDM1/BLIMP1, a sequence-specific regulator that is required for germ cell specification (Ohinata et al., 2005). Interestingly and uniquely, to our knowledge, PRDM14 is specifically expressed in defined windows during development (2- to 8-cell-stage embryos [this work], the epiblast, and primordial germ cells [Yamaji et al., 2008]), corresponding to critical periods of shifts in cellular potency and reprogramming. PRDM14 has been shown to function in repression as well as in activation of cell-specification genes and epigenetic regulators (Gillich et al., 2012; Ma et al., 2011; Yamaji et al., 2013). In ESCs, PRDM14 represses *Dnmt3b* and *Dnmt3l*, genes that show an inverse correlation to *Prdm14* expression in both 4-cell-stage embryos and blastocysts. Thus, it is likely that PRDM14 plays a role in repressing *Dnmt3b/3l* in the embryo.

The interaction with CARM1 that we uncovered, together with our observations that PRDM14 promotes global levels of H3R26me2 (an active chromatin mark) in the embryo, suggests that PRDM14 promotes ICM fate and pluripotency in vivo at least partially through the generation of a more open chromatin configuration, which is more typical of pluripotent cells (Meshorer et al., 2006). It is conceivable that at the 4-cell-stage, PRDM14, through its ZF domain, guides CARM1, which is expressed in a rather homogeneous fashion at this stage (data not shown; Torres-Padilla et al., 2007), to its target genes (Figure 7H). Thus, PRDM14 might promote stem cell fate allocation to the ICM both by favoring an open chromatin configuration and by repressing differentiation genes. This model is complementary to the proposed mechanism of action for promoting ground-state pluripotency by PRDM14 in ESCs in vitro through PRC2-mediated repression (Yamaji et al., 2013), which may apply at later stages in vivo, since *Ezh2* is weakly expressed before implantation (Figure S1). Further, we did not detect any effect of PRDM14 expression on H3K9me2 levels (Figure S7), a mode of PRDM14 action that was previously described in the germline (Yamaji et al., 2008; Magnúsdóttir et al., 2013). Likewise, PRDM14 dampens fibroblast growth factor receptor (FGFR) signaling to promote a primed pluripotency state in cultured ESCs (Yamaji et al., 2013). However, FGFR signaling is only important for later stages of development upon EPI and PE lineage restriction from the ICM, and does not affect the initial specification of the ICM itself (Chazaud et al., 2006; Kang et al., 2013). Together, these findings suggest that the mechanism of action of PRDM14 might differ depending on the cell type in which it is expressed, highlighting the importance of addressing PRDM14 function in its native context.

Lineage allocation is likely to involve a multicomponent cellular process, perhaps including stochastic decisions. Therefore, PRDM14 most probably does not play a master regulator role in lineage allocation, but rather acts as one component of a pathway that is involved in specification toward lineages that give rise to proportionally more ICM than TE cells. Thus, it seems that the forced expression of *Prdm14* does not alter the intrinsic process of differentiation per se, but biases the cells in which it is expressed at higher levels to fall into one fate pathway. The contribution of stochastic changes in gene expression to patterning of the early embryo (Dietrich and Hiiragi, 2007; Tabansky et al., 2013) is also compatible with this conclusion.

An important conclusion of our analysis is that the ICM and TE can be demarcated on the sole basis of the combination of the chromatin modifiers that they express. This implicates a distinct chromatin structure in these two lineages (Ahmed et al., 2010; Alder et al., 2010). The fact that ICM cells do not cluster together as well as TE cells indicates that ICM cells show more variability in the chromatin modifiers they express. This is consistent with the suggestion that cells that have not yet undergone a cell-fate decision (ICM cells) display a higher "transcriptional noise" than those that have already undergone cell-fate specification (TE cells).

Lastly, we find that 8-cell-stage blastomeres are most similar to TE cells of the blastocyst. This is particularly surprising because it suggests that 8-cell-stage blastomeres are more similar to TE cells than to their closest developmental stages in their epigenetic constituents. In contrast, in a similar analysis focusing on expression patterns of TFs (Guo et al., 2010), the 8-cell-stage blastomeres clustered with the ICM cells of the blastocyst. This implies that the similarity between the 8-cell-stage and TE cells of the blastocyst stems from the chromatin landscape. Indeed, removal of just three genes (*Kdm5a*, *Kdm6a*, and *Dnmt3l*) from the data set results in a loss of their clustering in the PCA. Because a differentiation process is initiated in both of these cell types, it is tempting to speculate that the three genes identified (*Kdm5a*, *Kdm6a*, and *Dnmt3l*) may play a functional role in initiating differentiation at both of these stages. Indeed, both *Kdm5a* (*Rbp2*) and *Kdm6a* (*Utx*) have been shown to promote differentiation in other systems (Agger et al., 2007; Lan et al., 2007; Lopez-Bigas et al., 2008), and DNA methylation is necessary to allow differentiation and contribution to the EPI lineages (Sakaue et al., 2010).

In summary, we have shown that a quantitative analysis of the expression of chromatin modifiers in single cells reveals a pattern of developmental transitions in the embryo and can predict cellular differentiation states. Importantly, we have identified PRDM14 as a regulator of cell-fate allocation. We propose that the combinatorial expression of chromatin modifiers defines cellular differentiation states and transitions in potency.

EXPERIMENTAL PROCEDURES

Embryo Collection

Embryos were collected from natural matings. Single oocytes, zygotes, or blastomeres were washed in PBS and flash-frozen in liquid nitrogen in 5 μl 2× reaction buffer.

All animal work was performed in accordance with the current legislation in France and with the approval of the regional ethics committee (COMETH).

High-Throughput Single-Cell qPCR

TaqMan Gene Expression Assays (Applied Biosystems) were pooled to a final concentration of 0.2×. For detailed reaction conditions, see Supplemental Experimental Procedures. Cell lysis and sequence-specific reverse transcription were performed at 50°C, followed by sequence-specific preamplification. The resulting cDNA was diluted 5-fold and analyzed in 48:48 dynamic arrays on a Biomark System (Fluidigm).

Raw Data Treatment and Visualization

All raw cycle threshold (Ct) values were normalized to the Ct detection level of 28. Ct values were further normalized by subtracting the respective Actin and RPLP0 as described by Guo et al. (2010). For visualization purposes, this normalization was omitted for Figures 1D–1F, 5C, and S1. PCA was performed on normalized Ct values using the svd command in R. Hierarchical clustering was performed using the Euclidean distances, and dendrograms were displayed along row-scaled heatmaps using the gplots package.

Single-Cell qPCR Validation

Validation was performed on single cells without preamplification collected in 5 μl 2× reaction buffer as described above on a LightCycler 480 Real-Time PCR System (Roche).

Embryo Microinjection and Culture

One blastomere of 2-cell-stage embryos was microinjected with capped hemagglutinin (HA)-tagged PRDM14 mRNA in combination with mRNA for GFP. Prdm14ΔZF comprises 1–1,104 bp of *mPrdm14*, and Prdm14ΔPR corresponds to fragments 1–718 and 1,086–1,686 bp of *mPrdm14*.

Immunofluorescence and Confocal Analysis of Embryos

Embryos were processed as described previously (Torres-Padilla et al., 2006). The antibodies used were anti-HA (Roche), anti-H3R26me2 (07-215; Millipore), anti-Dnmt3b (184A; Imgenex), anti-KDM5A (3876P; Cell Signaling), anti-PRMT2 (ARP40196; Aviva), anti-H3K9me2 (07-441; Millipore), and anti-PRDM14 (Reinberg laboratory).

Generation of the Map for an Epigenetic Landscape

In order to construct an epigenetic landscape, we first determined the number and location of the minima (valleys or wells) and the qualitative features of the corresponding graph (Bhattacharya et al., 2011). For a thorough explanation, see Supplemental Experimental Procedures.

Immunoprecipitation

Immunoprecipitation was performed with affinity-purified polyclonal PRDM14 antibody (antibody characterization is shown in Figure S6) and immunoblotting with anti-Carm1 (09-818; Millipore).

SUPPLEMENTAL INFORMATION

Supplemental Information includes Supplemental Experimental Procedures, seven figures, eight tables, and two movies and can be found with this article online at http://dx.doi.org/10.1016/j.celrep.2013.09.044.

ACKNOWLEDGMENTS

We thank D. Reinberg for the PRDM14 antibody, and the imaging and animal facilities of the IGBMC for support. M.-E.T.-P. received funding from AVENIR/INSERM, ANR-09-Blanc-0114, EpiGeneSys FP7 NoE, and an ERC-Stg grant ("NuclearPotency"). A.B. received a postdoctoral fellowship from the Fondation pour la Recherche Médicale and an EMBO short-term fellowship (ASTF 54.00 2011). E.G. and J.M. acknowledge funding from ASTAR JCO (grant-1134c001) and A-STAR core funding to the IMCB.

Received: April 5, 2013
Revised: August 16, 2013
Accepted: September 28, 2013
Published: October 31, 2013

REFERENCES

Agger, K., Cloos, P.A., Christensen, J., Pasini, D., Rose, S., Rappsilber, J., Issaeva, I., Canaani, E., Salcini, A.E., and Helin, K. (2007). UTX and JMJD3 are histone H3K27 demethylases involved in HOX gene regulation and development. Nature *449*, 731–734.

Ahmed, K., Dehghani, H., Rugg-Gunn, P., Fussner, E., Rossant, J., and Bazett-Jones, D.P. (2010). Global chromatin architecture reflects pluripotency and lineage commitment in the early mouse embryo. PLoS ONE *5*, e10531.

Alder, O., Lavial, F., Helness, A., Brookes, E., Pinho, S., Chandrashekran, A., Arnaud, P., Pombo, A., O'Neill, L., and Azuara, V. (2010). Ring1B and Suv39h1 delineate distinct chromatin states at bivalent genes during early mouse lineage commitment. Development *137*, 2483–2492.

Bhattacharya, S., Zhang, Q., and Andersen, M.E. (2011). A deterministic map of Waddington's epigenetic landscape for cell fate specification. BMC Syst. Biol. *5*, 85.

Borgel, J., Guibert, S., Li, Y., Chiba, H., Schübeler, D., Sasaki, H., Forné, T., and Weber, M. (2010). Targets and dynamics of promoter DNA methylation during early mouse development. Nat. Genet. *42*, 1093–1100.

Bultman, S.J., Gebuhr, T.C., Pan, H., Svoboda, P., Schultz, R.M., and Magnuson, T. (2006). Maternal BRG1 regulates zygotic genome activation in the mouse. Genes Dev. *20*, 1744–1754.

Burton, A., and Torres-Padilla, M.E. (2010). Epigenetic reprogramming and development: a unique heterochromatin organization in the preimplantation mouse embryo. Brief Funct Genomics *9*, 444–454.

Chazaud, C., Yamanaka, Y., Pawson, T., and Rossant, J. (2006). Early lineage segregation between epiblast and primitive endoderm in mouse blastocysts through the Grb2-MAPK pathway. Dev. Cell *10*, 615–624.

Chen, D., Ma, H., Hong, H., Koh, S.S., Huang, S.M., Schurter, B.T., Aswad, D.W., and Stallcup, M.R. (1999). Regulation of transcription by a protein methyltransferase. Science *284*, 2174–2177.

Dietrich, J.E., and Hiiragi, T. (2007). Stochastic patterning in the mouse preimplantation embryo. Development *134*, 4219–4231.

Erhardt, S., Su, I.H., Schneider, R., Barton, S., Bannister, A.J., Perez-Burgos, L., Jenuwein, T., Kouzarides, T., Tarakhovsky, A., and Surani, M.A. (2003). Consequences of the depletion of zygotic and embryonic enhancer of zeste 2 during preimplantation mouse development. Development *130*, 4235–4248.

Gillich, A., Bao, S., Grabole, N., Hayashi, K., Trotter, M.W., Pasque, V., Magnúsdóttir, E., and Surani, M.A. (2012). Epiblast stem cell-based system reveals reprogramming synergy of germline factors. Cell Stem Cell *10*, 425–439.

Guo, G., Huss, M., Tong, G.Q., Wang, C., Li Sun, L., Clarke, N.D., and Robson, P. (2010). Resolution of cell fate decisions revealed by single-cell gene expression analysis from zygote to blastocyst. Dev. Cell *18*, 675–685.

Hamatani, T., Carter, M.G., Sharov, A.A., and Ko, M.S. (2004). Dynamics of global gene expression changes during mouse preimplantation development. Dev. Cell *6*, 117–131.

Hemberger, M., Dean, W., and Reik, W. (2009). Epigenetic dynamics of stem cells and cell lineage commitment: digging Waddington's canal. Nat. Rev. Mol. Cell Biol. *10*, 526–537.

Hirasawa, R., and Sasaki, H. (2009). Dynamic transition of Dnmt3b expression in mouse pre- and early post-implantation embryos. Gene Expr. Patterns *9*, 27–30.

Hirasawa, R., Chiba, H., Kaneda, M., Tajima, S., Li, E., Jaenisch, R., and Sasaki, H. (2008). Maternal and zygotic Dnmt1 are necessary and sufficient for the maintenance of DNA methylation imprints during preimplantation development. Genes Dev. *22*, 1607–1616.

Johnson, M.H. (2009). From mouse egg to mouse embryo: polarities, axes, and tissues. Annu. Rev. Cell Dev. Biol. *25*, 483–512.

Johnson, M.H., and McConnell, J.M. (2004). Lineage allocation and cell polarity during mouse embryogenesis. Semin. Cell Dev. Biol. *15*, 583–597.

Kang, M., Piliszek, A., Artus, J., and Hadjantonakis, A.K. (2013). FGF4 is required for lineage restriction and salt-and-pepper distribution of primitive endoderm factors but not their initial expression in the mouse. Development *140*, 267–279.

Lan, F., Bayliss, P.E., Rinn, J.L., Whetstine, J.R., Wang, J.K., Chen, S., Iwase, S., Alpatov, R., Issaeva, I., Canaani, E., et al. (2007). A histone H3 lysine 27 demethylase regulates animal posterior development. Nature *449*, 689–694.

Lopez-Bigas, N., Kisiel, T.A., Dewaal, D.C., Holmes, K.B., Volkert, T.L., Gupta, S., Love, J., Murray, H.L., Young, R.A., and Benevolenskaya, E.V. (2008). Genome-wide analysis of the H3K4 histone demethylase RBP2 reveals a transcriptional program controlling differentiation. Mol. Cell *31*, 520–530.

Lorthongpanich, C., Doris, T.P., Limviphuvadh, V., Knowles, B.B., and Solter, D. (2012). Developmental fate and lineage commitment of singled mouse blastomeres. Development *139*, 3722–3731.

Ma, Z., Swigut, T., Valouev, A., Rada-Iglesias, A., and Wysocka, J. (2011). Sequence-specific regulator Prdm14 safeguards mouse ESCs from entering extraembryonic endoderm fates. Nat. Struct. Mol. Biol. *18*, 120–127.

Magnúsdóttir, E., Dietmann, S., Murakami, K., Günesdogan, U., Tang, F., Bao, S., Diamanti, E., Lao, K., Gottgens, B., and Azim Surani, M. (2013). A tripartite transcription factor network regulates primordial germ cell specification in mice. Nat. Cell Biol. *15*, 905–915.

Meshorer, E., Yellajoshula, D., George, E., Scambler, P.J., Brown, D.T., and Misteli, T. (2006). Hyperdynamic plasticity of chromatin proteins in pluripotent embryonic stem cells. Dev. Cell *10*, 105–116.

Mitsui, K., Tokuzawa, Y., Itoh, H., Segawa, K., Murakami, M., Takahashi, K., Maruyama, M., Maeda, M., and Yamanaka, S. (2003). The homeoprotein Nanog is required for maintenance of pluripotency in mouse epiblast and ES cells. Cell *113*, 631–642.

Nichols, J., Zevnik, B., Anastassiadis, K., Niwa, H., Klewe-Nebenius, D., Chambers, I., Schöler, H., and Smith, A. (1998). Formation of pluripotent stem cells in the mammalian embryo depends on the POU transcription factor Oct4. Cell *95*, 379–391.

Ohinata, Y., Payer, B., O'Carroll, D., Ancelin, K., Ono, Y., Sano, M., Barton, S.C., Obukhanych, T., Nussenzweig, M., Tarakhovsky, A., et al. (2005). Blimp1 is a critical determinant of the germ cell lineage in mice. Nature *436*, 207–213.

Okano, M., Bell, D.W., Haber, D.A., and Li, E. (1999). DNA methyltransferases Dnmt3a and Dnmt3b are essential for de novo methylation and mammalian development. Cell *99*, 247–257.

Parfitt, D.E., and Zernicka-Goetz, M. (2010). Epigenetic modification affecting expression of cell polarity and cell fate genes to regulate lineage specification in the early mouse embryo. Mol. Biol. Cell *21*, 2649–2660.

Puschendorf, M., Terranova, R., Boutsma, E., Mao, X., Isono, K., Brykczynska, U., Kolb, C., Otte, A.P., Koseki, H., Orkin, S.H., et al. (2008). PRC1 and Suv39h specify parental asymmetry at constitutive heterochromatin in early mouse embryos. Nat. Genet. *40*, 411–420.

Ratnam, S., Mertineit, C., Ding, F., Howell, C.Y., Clarke, H.J., Bestor, T.H., Chaillet, J.R., and Trasler, J.M. (2002). Dynamics of Dnmt1 methyltransferase expression and intracellular localization during oogenesis and preimplantation development. Dev. Biol. *245*, 304–314.

Rossant, J., and Tam, P.P. (2009). Blastocyst lineage formation, early embryonic asymmetries and axis patterning in the mouse. Development *136*, 701–713.

Sakaue, M., Ohta, H., Kumaki, Y., Oda, M., Sakaide, Y., Matsuoka, C., Yamagiwa, A., Niwa, H., Wakayama, T., and Okano, M. (2010). DNA methylation is dispensable for the growth and survival of the extraembryonic lineages. Curr. Biol. *20*, 1452–1457.

Strumpf, D., Mao, C.A., Yamanaka, Y., Ralston, A., Chawengsaksophak, K., Beck, F., and Rossant, J. (2005). Cdx2 is required for correct cell fate specification and differentiation of trophectoderm in the mouse blastocyst. Development *132*, 2093–2102.

Tabansky, I., Lenarcic, A., Draft, R.W., Loulier, K., Keskin, D.B., Rosains, J., Rivera-Feliciano, J., Lichtman, J.W., Livet, J., Stern, J.N., et al. (2013). Developmental bias in cleavage-stage mouse blastomeres. Curr. Biol. *23*, 21–31.

Tang, F., Barbacioru, C., Nordman, E., Bao, S., Lee, C., Wang, X., Tuch, B.B., Heard, E., Lao, K., and Surani, M.A. (2011). Deterministic and stochastic allele specific gene expression in single mouse blastomeres. PLoS ONE *6*, e21208.

Torres-Padilla, M.E., Bannister, A.J., Hurd, P.J., Kouzarides, T., and Zernicka-Goetz, M. (2006). Dynamic distribution of the replacement histone variant H3.3 in the mouse oocyte and preimplantation embryos. Int. J. Dev. Biol. *50*, 455–461.

Torres-Padilla, M.E., Parfitt, D.E., Kouzarides, T., and Zernicka-Goetz, M. (2007). Histone arginine methylation regulates pluripotency in the early mouse embryo. Nature *445*, 214–218.

Wang, Q.T., Piotrowska, K., Ciemerych, M.A., Milenkovic, L., Scott, M.P., Davis, R.W., and Zernicka-Goetz, M. (2004). A genome-wide study of gene activity reveals developmental signaling pathways in the preimplantation mouse embryo. Dev. Cell *6*, 133–144.

Yamaji, M., Seki, Y., Kurimoto, K., Yabuta, Y., Yuasa, M., Shigeta, M., Yamanaka, K., Ohinata, Y., and Saitou, M. (2008). Critical function of Prdm14 for the establishment of the germ cell lineage in mice. Nat. Genet. *40*, 1016–1022.

Yamaji, M., Ueda, J., Hayashi, K., Ohta, H., Yabuta, Y., Kurimoto, K., Nakato, R., Yamada, Y., Shirahige, K., and Saitou, M. (2013). PRDM14 ensures naive pluripotency through dual regulation of signaling and epigenetic pathways in mouse embryonic stem cells. Cell Stem Cell *12*, 368–382.

Ziomek, C.A., and Johnson, M.H. (1980). Cell surface interaction induces polarization of mouse 8-cell blastomeres at compaction. Cell *21*, 935–942.